



Published by Avanti Publishers  
**The Global Environmental  
Engineers**

ISSN (online): 2410-3624



## Unraveling the Potential of Micro-nano Bubbles in Water Treatment: A Review Focusing on Physicochemical Properties, Generation Methods, and Environmental Impacts

Ling Li <sup>1,2</sup>, Honglin Liu <sup>1,2</sup>, Yingping Huang <sup>1,2</sup>, Feng Hong <sup>1,2</sup>, Xi Yuan <sup>1,2,\*</sup>, Wei Cai<sup>3</sup>,  
Chuncheng Chen <sup>4</sup> and Di Huang <sup>2,\*</sup>

<sup>1</sup>College of Hydraulic and Environmental Engineering, China Three Gorges University, Yichang 443002, Hubei, China

<sup>2</sup>Engineering Research Center of Eco-Environment in Three Gorges Reservoir Region, China Ministry of Education, Three Gorges University, Yichang 443002, Hubei, China

<sup>3</sup>China Yangtze Power Co., Ltd., Yichang 443002, China

<sup>4</sup>Beijing National Laboratory for Molecular Sciences, Key Laboratory of Photochemistry, CAS Research/Education Center for Excellence in Molecular Sciences, Institute of Chemistry, Chinese Academy of Sciences, Beijing 100190, China

### ARTICLE INFO

Article Type: Review Article

Academic Editor: Tao Wang 

Keywords:

Mass transfer

Micro-nano bubbles

Wastewater treatment

Advanced oxidation processes

Reactive oxygen species generation

Timeline:

Received: October 30, 2024

Accepted: December 02, 2024

Published: December 15, 2024

Citation: Li L, Liu H, Huang Y, Hong F, Yuan X, Cai W, Chen C, Huang D. Unraveling the potential of micro-nano bubbles in water treatment: A review focusing on physicochemical properties, generation methods, and environmental impacts. Glob Environ Eng. 2024; 11: 37-53.

DOI: <https://doi.org/10.15377/2410-3624.2024.11.3>

\*Corresponding Author

Email: [huangyp@ctgu.edu.cn](mailto:huangyp@ctgu.edu.cn)

Tel: +(86) 13872539594

### ABSTRACT

With the advancement of industrialization, water pollution has become a pressing global environmental issue. Traditional water treatment technologies are struggling to remove emerging contaminants and meet current discharge standards, against this backdrop, micro-nano bubbles (MNBs) technology has attracted considerable research attention due to its unique physicochemical properties, such as long-term stability, high internal pressure, photoelectric characteristics, and reactive oxygen species (ROS) generation capabilities, especially in its combination with advanced oxidation processes (AOPs). A comprehensive understanding of MNBs generation and utilization is significant for developing green, economical, and highly effective wastewater treatment technologies. Herein, on the basis of the comprehensive literature survey, this review article systematically studied the distinctive characteristics of MNBs, along with the methodologies employed for their generation. It concurrently explores the characterization methods used to assess the properties of MNBs, which is instrumental for subsequent analyses on how these properties can enhance the catalytic performance of AOPs. Finally, this article explores the potential applications of MNBs in the environmental sector and points out the direction for future research, including the development of more efficient and cost-effective MNBs generation technologies, in-depth exploration of their mechanisms in AOPs, and comprehensive environmental impact assessments. This review aims to provide readers with an in-depth understanding of the intrinsic correlation between the properties and applications of MNBs, thereby enabling their optimal utilization in the environmental remediation.

## 1. Introduction

As industrialization advances and the population expands, water pollution has emerged as a pressing global environmental issue. The pervasive presence of interfering substances, such as inorganic anions in aquatic systems, coupled with the introduction of emerging pollutants, has rendered traditional treatment methodologies inadequate for meeting current discharge standards [1-6]. Consequently, the development of environmentally friendly and highly effective wastewater treatment technologies has become an important focus in the field of environmental science.

In this context, technology based on micro-nano bubbles (MNBs) has garnered widespread attention due to the unique physicochemical properties. MNBs, defined as bubbles with a diameter less than 1  $\mu\text{m}$ , exhibit a range of distinct characteristics such as long-term stability, high internal pressure, photoelectric properties, and reactive oxygen species (ROS) generation capabilities [7-9]. These properties make MNBs very promising for wastewater treatment, especially within advanced oxidation processes (AOPs). For example, due to the balance between surface forces such as electrostatic repulsion and van der Waals attraction, the high stability of MNBs allows them to persist in liquids for extended periods, thereby enabling sustained release of reactive substances and prolonging treatment efficacy [10-12]. Besides, the small size of MNBs endows them with an exceptionally large surface area to volume ratio, which intensifies mass transfer at the liquid-gas interface and enhances the interaction between the bubbles and oxidants or pollutants [13-15]. Moreover, leveraging the optoelectronic properties of MNBs can enhance the efficiency of photocatalytic reactions, where the bubbles serve as microreactors, facilitating the separation and transfer of photogenerated charge carriers [16, 17]. However, despite the potential demonstrated by MNBs in enhancing catalytic efficiency, debates persist regarding their specific reaction mechanisms. Some studies suggested that MNBs may improve the utilization rate of ozone and oxygen by increasing mass transfer efficiency at the gas-liquid interface and the solubility of gases [18, 19], while others focused on the process of  $\cdot\text{OH}$  generation induced by the collapse of MNBs [20-22]. These studies offer varying perspectives to explain the reaction mechanisms of MNBs, yet a unified theory has not been established.

The generation and application of MNBs constitute an interdisciplinary research field, encompassing physical chemistry, materials science, environmental engineering, and more [11, 23]. The preparation methods and characterization of MNBs are also crucial for their environmental applications. Currently, the primary methods for generating MNBs include electrolysis, hydrodynamic cavitation, acoustic cavitation, and solvent exchange, etc. [24-27]. Each of these methods has its own set of advantages and disadvantages, and the appropriate method must be selected based on considerations of efficiency, cost, and ease of operation. For instance, electrolysis can produce a high concentration of MNBs but with higher energy consumption [28, 29], while solvent exchange is a low-cost method that generates a lower concentration of bubbles [11]. Therefore, researchers need to choose the most suitable generation method based on specific application requirements.

So far, numerous reviews have summarized the preparation, mass transport and stability theories of MNBs [7, 10, 30], along with their applications in the oxidation of emerging contaminants [9, 28, 31], membrane cleaning [10, 29], flotation processes [7, 32], and adsorption techniques [32, 33]. These reviews have significantly advanced the application of MNBs. By studying these literatures and the recently published works, we further analyze the advantages and disadvantages of MNBs generation methods and characterization methods to assist in the selection of appropriate application scenarios. However, there is still lack of studies focusing on the delaying mechanisms by which MNBs function within AOPs. Therefore, in this critical review, the unique properties of MNBs are also introduced with a focus on those that may significantly influence the catalytic efficiency of AOPs. The efficiency of MNBs-assisted ozonation process, Fenton-like process, and photocatalytic process for water decontamination are also discussed. Finally, the challenges and further research needs for MNBs-assisted AOPs in the wastewater treatment are pointed out.

## 2. Physicochemical Properties of MNBs

In solutions, bubbles are generally classified into three categories based on their diameter: macrobubbles (diameter > 100  $\mu\text{m}$ ), microbubbles (diameter = 1-100  $\mu\text{m}$ ), and nanobubbles (diameter < 1  $\mu\text{m}$ ) (Fig. **1A**) [10, 32].

Relative to macrobubbles, MNBs exhibit smaller diameters and possess a range of distinct physicochemical properties, such as long-term stability, high internal pressure, Photoelectric characteristics and ROS generation, etc.

## 2.1. Long-term Stability

The ascent velocity of a bubble within a liquid is directly proportional to the square of the bubble's diameter. Consequently, compared with macrobubbles, the residence time of MNBs in solution is significantly extended, and it can be stable in liquid for a long time (from days to months) [31, 34], which is advantageous for enhancing mass transfer. Meanwhile, it has been reported that the surface zeta potential of MNBs is negative in an alkaline medium [28, 33, 35]. This negative charge facilitates electrostatic repulsion among MNBs, thereby impeding their coalescence and enhancing their colloidal stability within the solution. Conversely, under acidic conditions, the negative surface charge on the MNBs may be neutralized [9], which diminishes the electrostatic repulsive forces between them, consequently compromising their diameter in the solution. For example, Prakash *et al.* [36] reported that the average diameter of MNBs was larger in acidic media (pH < 7) compared to alkaline media (pH > 7), and the largest diameter was observed at pH 4.5 (Fig. **1B**). That is to say, the stability of MNBs can be modulated by adjusting the solution pH. Hence, in the process of water treatment using MNBs, it is also essential to closely monitor the impact behavior of solution pH.

## 2.2. High Internal Pressure

The contribution of surface tension to the internal pressure of a bubble is inversely proportional to the bubble's diameter. Consequently, a reduction in the bubble's diameter leads to an increased pressure exerted by the water's surface tension on the bubble's interior, which in turn elevates the partial pressure of the gas contained within the bubble [37, 38]. For example, findings from synchrotron radiation scanning transmission X-ray microscopy have demonstrated that the surface oxygen density of individual nanobubbles is significantly higher, by 1-2 orders of magnitude, compared to that under standard atmospheric conditions [39]. The differential pressure between the interior of MNBs and the surrounding aqueous solution facilitates an enhanced transfer efficiency of gas from the bubble to the aqueous phase [40, 41]. Additionally, the high internal pressure enables MNBs to generate a localized high-pressure environment during their collapse. This high-pressure environment may exert mechanical forces on catalysts within the system, inducing deformation and consequently leading to a relative displacement of the internal centers of positive and negative charges, which in turn results in the generation of a built-in electric field and facilitates electron transfer process. However, there are few studies on the localized high-pressure environment generated during the collapse of MNBs inducing the catalysts to generate built-in electric fields. Further studies are needed to reveal the intrinsic mechanism to better utilize the local high-pressure environment generated during MNBs collapse.

## 2.3. Photoelectric Characteristics

Owing to the pronounced discrepancies in refractive indices and optical properties between air and liquids, solutions with entrapped gas bubbles demonstrate distinctive optical characteristics, notably light scattering (Fig. **1C**) [16, 42]. This scattering is inversely related to the bubble size, with smaller bubbles exhibiting more pronounced scattering effects. Consequently, MNBs possess a higher single-scattering albedo, and it can elongate the optical path length within specific regions proximate to the light source in a solution [43-45]. This elongation results in an increased optical density (OD), which aids in enhancing the light absorption capacity of photocatalysts and, by extension, promotes photocatalytic reactions. Fan *et al.* simulated the electrical intensity ( $|E|^2$  representing the optical intensity) of water alone, single Ag/TiO<sub>2</sub> particle, single spore, single MNBs, and Ag/TiO<sub>2</sub> particle placed at the surface of the spore with an MNBs placed closely to the spore by utilizing finite difference time domain (FDTD) model. As can be seen from Fig. (**1D**), light intensity was maximized at the bubble edge and divergence paths, MNB presence enhanced the electric field in these regions up to fourfold the incident light intensity [17]. However, research on leveraging the optical properties of MNBs to enhance photocatalytic reactions is currently limited. As bubble optics theory continues to evolve, some related mechanisms, such as how the concentration of MNBs and the conditions of complex aqueous environments affect the light-scattering behaviors in the presence of MNBs, and thus photocatalytic efficiencies, need to be further investigated.

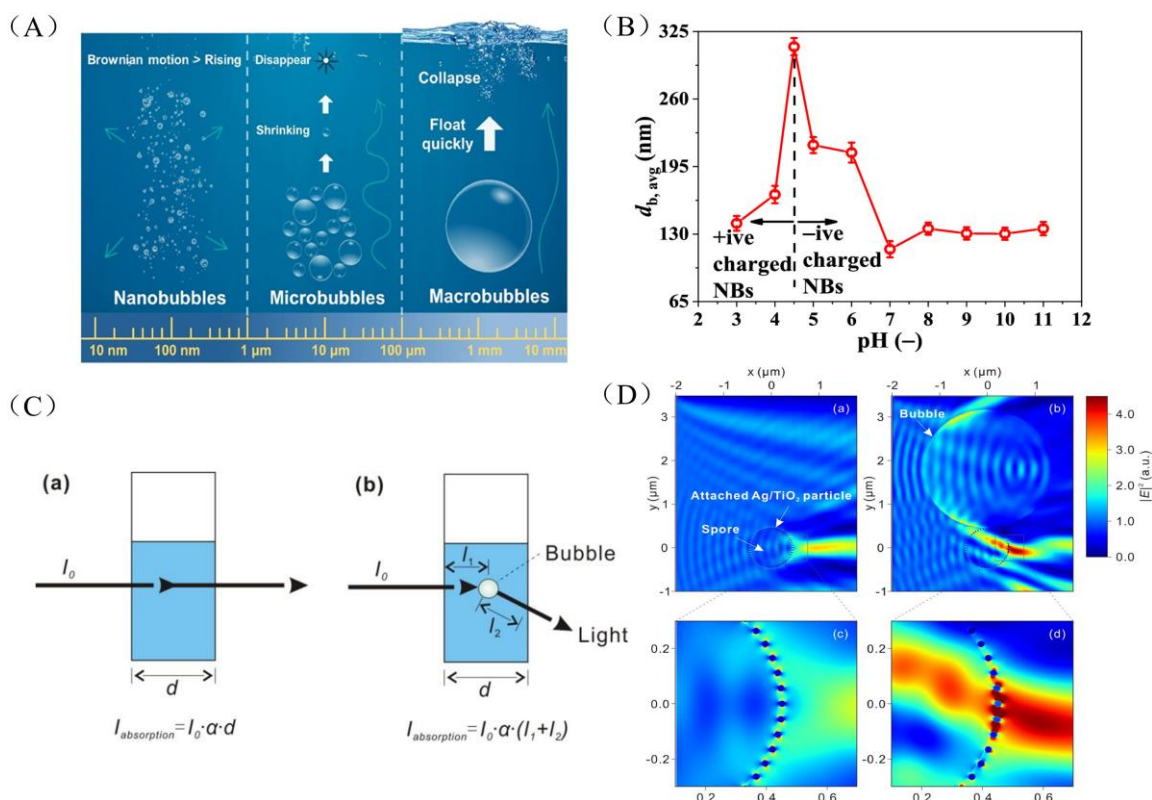


**Figure 1:** (A) The schematic diagram of nanobubbles, microbubbles, and macrobubbles [9]; (B) The variation of average diameter of nanobubbles with solution pH [36]; (C) The diagram of light propagation and optical path length in the presence and absence of bulk bubbles [45]; and (D) Electric field distribution near an illuminated spore with attached Ag/TiO<sub>2</sub> particles, an illuminated MNB with a nearby Ag/TiO<sub>2</sub> particles coated spore and the corresponding enlarged images [17].

## 2.4. ROS Generation

Previous researches have documented that during the collapse of MNBs, charge ions are rapidly concentrated and enriched on the extremely narrow bubble interface, resulting in a significant increase in zeta potential. Before the MNBs burst, a very high zeta potential value can be formed at the interface, thereby generating a local electric field [46, 47]. Meanwhile, upon the collapse of MNBs, the surrounding fluid rapidly infiltrates the vacated volume. The associated swift fluidic motion induces shear forces, which can lead to the dissociation of charges, thereby amplifying the local electric field. And this localized high temperature and pressure and electric field changes during MNBs collapse may further induce the generation of ROS [11, 20, 31]. However, current researches have primarily demonstrated that the collapse of MNBs could produce ROS, and there is an urgent need for more studies to elucidate the underlying mechanisms to maximize the utilization of MNBs in enhancing the catalytic efficiency of catalytic reactions.

## 3. Generation and Characterization of MNBs

Due to the specific properties of MNBs, such as high stability and the ability to enhance mass transfer efficiency, they are highly beneficial in wastewater treatment processes. Consequently, some studies have begun to explore various methods, including electrolysis, hydrodynamic cavitation, acoustic cavitation, and solvent exchange, etc. to improve the efficiency of MNBs generation [10, 25, 28, 29, 48]. Understanding the principles of these methods helps in selecting the appropriate means to produce MNBs. Furthermore, after the generation of MNBs, it is significant to confirm their existence and to verify their size and surface properties through certain characterization techniques [29, 49]. Therefore, in this section, we will summarize some common methods for MNBs generation and characterization techniques for examining their structural properties.

### 3.1. Generation Methods

#### 3.1.1. Electrolysis

The evolution of MNBs during the electrocatalytic process is related to classical nucleation theory, which includes three steps: nucleation, growth, and detachment (Fig. **2A**) [25, 50, 51]. To be specific, the electrode surfaces of most electrocatalytic reactions often involve the formation or consumption of gas molecules, resulting in the formation of a high concentration of gas molecules around electrode surface. Within these regions, gas molecules spontaneously form gas embryos, which are dense collections of gas molecules. These gas embryos are in a metastable state, with the dense collections of gas molecules continuously undergoing spontaneous dissolution and aggregation. As the reaction progresses, the gas embryos either merge with themselves or with surrounding molecules to form nanoscale clusters. When these clusters acquire the necessary activation energy and overcome the phase transition barrier, they form gas nuclei. After nucleation, since the diffusion rate of gas molecules from solution into the bubbles exceeds the rate at which they diffuse from the bubbles back into solution, the bubbles begin to grow. Then the bubbles will begin to detach from the electrode surface after growing to a certain size. In addition, it is worth noting that bubbles tend to form at heterogeneous interfaces (such as cracks on the electrode surface or impurities in the liquid phase).

Linde *et al.* investigated the diffusion-driven growth kinetics of H<sub>2</sub> bubbles generation on silicon electrode substrate (Fig. **2B**). They found that for a certain range of current densities (5-15 A/m<sup>2</sup>), the H<sub>2</sub> bubbles evolution first underwent a stagnation period, followed by a rapid increase in the growth coefficient, and finally reached a steady state [52]. Jadhav *et al.* investigated the nanobubbles generation under different solution pH. It was found that the nanobubbles existed as stable cluster under alkaline condition, but dissociated into tiny primary nanobubbles of about 1 nm under neutral and acidic conditions. Besides, the experimental results showed that a higher electrolyte concentration, longer operating time, greater current input, or lower water operating temperature was beneficial for the generation of nanobubbles [50]. Overall, the generation of MNBs through electrocatalytic process offers the advantage of precise control over bubble quantity and size through adjustable electrolysis conditions, enhancing application flexibility and precision.

Nevertheless, bubble adsorption and blockage on electrodes during electrolysis can impair efficiency and electrode performance, requiring periodic maintenance. This challenge restricts the stability of the electrolysis method for broader applications. In order to improve the stability of electrocatalytic MNBs generation systems, many researchers have focused on researching ways to reduce the adhesion force of MNBs. For example, Zhang *et al.* found that both nanobubbles adhesion and nanobubbles detachment were related to current density. They successfully predicted the critical current density for a stable nanobubble based on stability theory for surface nanobubbles. By adjusting the current density, they enhanced the bubble detachment, thereby enhancing the stability of electrolysis and bubble generation [53]. Similarly, superhydrophobic nanoarray electrodes have been reported to significantly reduce the adhesion of MNBs [54-56], thereby reducing catalyst stripping from the electrode surface and improving the stability of the electrocatalytic system in the presence of MNBs. In addition to bubble blockage, the application of electrolysis in the industrial production of MNBs is also limited due to the technical complexity of electrolysis, such as the selection of electrode materials and the optimization of electrolyte.

#### 3.1.2. Cavitation

Cavitation arises when the pressure in a fluid system is decreased to values below a critical threshold [11, 32, 57-59]. This phenomenon can be induced by two primary methods: one involves the use of hydraulic devices to increase the flow velocity (such as hydrodynamic cavitation), which leads to changes in the pressure of the flowing liquid [48, 57]; and the other involves the input of energy to cause local pressure fluctuations (such as acoustic cavitation) [32, 60, 61].

##### 3.1.2.1. Hydrodynamic Cavitation

When the pressure at a point within a liquid momentarily decreases below its vapor pressure due to excessively high velocity, hydrodynamic cavitation occurs [27, 62]. It is characterized by minimal maintenance

requirements and cost-effective scalability, rendering it one of the most economical and energy-efficient approaches for cavitation induction. Currently, the primary methods for generating MNBs through hydrodynamic cavitation include depressurization of gas-saturated liquids through a flow constrictor [59, 62, 63], spiral flow/rotary flow/swirl method [19, 58, 64], and pressure dissolution/pressurization decompression [65, 66].

(1) The process of depressurizing gas-saturated liquids is commonly facilitated by employing a flow constrictor, with the Venturi tube being the most prevalent apparatus for this purpose. Within the conical convergence zone of a Venturi tube, the liquid flow experiences acceleration as it traverses the narrowing diameter. Consequently, the liquid flow rate at the throat is significantly higher compared to that at the inlet cylinder, while the pressure correspondingly decreases below the vapor pressure of the liquid, thereby inducing cavitation (Fig. 2C) [48]. Zhou *et al.* investigated the impact of preparation time and aeration rate on the properties of MNBs generated using a Venturi tube. The findings revealed that the increase of preparation time and aeration related to the decrease of microbubbles number, while the concentration of nanobubbles initially increased and then decreased. Additionally, it was observed that the electronegativity of nanobubbles diminished with an escalation in the aeration rate [48]. In our previous studies, the cavitation intensity within a Venturi cavitation device was predicted through a robust CFD computational method coupling with the Gilmore-NASG bubble dynamic model (Fig. 2D), which facilitated the effective comparison and assessment of bubble dynamics and cavitation intensity in the multiphase flow of cavitation reactors [63]. In short, the Venturi tube, with its simple structure, low operating costs, and resistance to blockage, is well-suited for the industrial production of MNBs. However, the method usually results in a non-uniform size distribution of MNBs, necessitating further improvements for enhanced uniformity and control over bubble size.

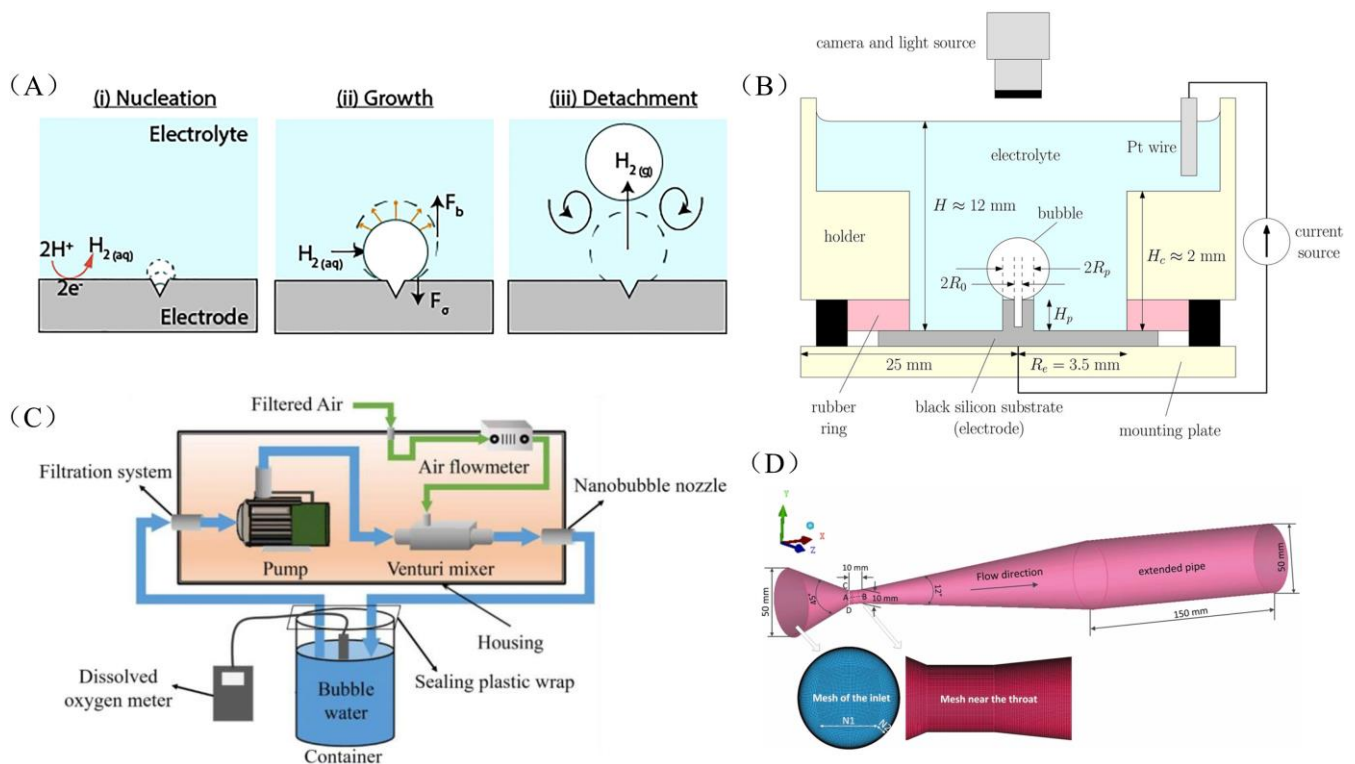


**Figure 2:** (A) The various stages of bubble evolution during electrolysis [25]; (B) The sketch of electrolysis setup for bubble generation [52]. (C) The working principle of the fine-bubbles generator [48]; and (D) Computational domain and local mesh distribution of venturi tube [63].

(2) For spiral flow/rotary flow/swirl method, upon pumping water into the generator, the liquid flow undergoes high-speed rotation, generating a vortex-like cavity that results in the formation of a surrounding low-pressure zone. MNBs are nucleated once the pressure in this zone decreases below the vapor pressure of the liquid. Jain *et al.* utilized both orifice and vortex diode cavitation devices to generate MNBs (Fig. 3A) [64]. The vortex

diode cavitation device was found to be more user-friendly and significantly more efficient. The cavitation effect was induced within a cylindrical swirling chamber. As water passed through the swirling chamber, it formed a vortex jet. The central pressure of this jet was lower than the vapor pressure of water, thereby leading to the formation of MNBs. Similar to the issues encountered with Venturi tubes, the generation of MNBs using spiral/rotary/vortex flow methods also suffers from the problem of non-uniform bubble size distribution, which necessitates further improvement.

- (3) The pressure alteration technique for the generation of MNBs is predicated on Henry's law. This process involves the dissolution of a gas in water under elevated pressure to achieve saturation. Upon the abrupt release of pressure, the solubility of the gas diminishes, precipitating MNBs from the aqueous solution. The reciprocating differential pressure method manipulates the pressure within a syringe by the oscillatory movement of a piston, facilitating the formation of MNBs. The concentration of MNBs can be precisely regulated by modulating the frequency of the piston's reciprocating motion. As reported by Ferraro *et al.*, by performing continuous expansion/compression strokes within a sealed syringe, a stable block of nanobubbles with a concentration exceeding  $10^9$  bubbles  $\text{mL}^{-1}$  was generated in pure water (Fig. **3B**) [65]. Overall, generating MNBs through the pressure alteration technique offers the advantages of a simple structure and low operational costs. However, it also faces issues such as low energy utilization efficiency and low efficiency in micro-nanobubble generation, as well as deficiencies in equipment stability.

### 3.1.2.2. Acoustic Cavitation

Acoustic cavitation is also a common and convenient method for generating MNBs. Taking ultrasonic waves as an example, ultrasonic waves consist of a series of horizontal and vertical mechanical waves that propagate uniformly through the solution, causing fluctuations of high and low pressure within the liquid. During the low-pressure phase, the internal pressure of the liquid decreases. When the pressure is reduced below the saturated vapor pressure, cavitation nuclei formed by microbubbles, solid particles, or other tiny structures within the liquid will begin to grow, forming MNBs (Fig. **3C**). Additionally, MNBs may also form in the vicinity of collapsing bulk bubbles [23, 24, 60, 61]. Some researchers have reported that MNBs can be generated by a 42 kHz Branson Ultrasonic Cleaner Model [67], a Langevin transducer with multiple frequencies (HEC45242M, Honda Electronics) [68], a 20 kHz Vibra-Cell sonicator (Sonic & Material Instrument) [69], a 20 kHz probe-type US processor (AUTOTUNE SERIES 750 W and 1500 W model, Sonics & Materials) [70], and a frequency of 40 kHz ultrasound (no manufacturer information) [24]. Besides, it is noted that ultrasound parameters, such as frequency and intensity significantly influence cavitation effects and the formation of MNBs [23, 71]. For instance, Mo *et al.* investigated the impact of ultrasonication time on the concentration of nanobubbles. The results indicated that the concentration of nanobubbles reached a maximum when the ultrasonication time was extended to approximately 1 min. With the extension of ultrasonic time to 3 to 10 min, the concentration of nanobubbles decreased slightly, while the average diameter increased slightly [24]. However, despite the extensive researches on the generation of MNBs through ultrasonic cavitation, the process is typically accompanied by high energy consumption, which constrains its application in practical engineering scenarios.

### 3.1.3. Solvent Exchange

MNBs generation through solvent exchange is based on the difference in solubility of gases in different solutions (Fig. **3D**). This method requires that the two solutions can be mixed in any proportion and that the solubility of the same gas in the two solutions is significantly different. Due to the difference in gas solubility in the solutions, local supersaturation occurs during the solution exchange process, leading to bubble nucleation and thus the preparation of MNBs [26, 72, 73]. The most frequently employed solvent pairs for this method include aqueous and ethanolic solutions, aqueous and saline solutions, and cold and hot water mixtures. In terms of repeatability and stability, the ethanol-water substitution is predominantly utilized. By modulating the ratio of ethanol to water, this technique enables the production of MNBs with varying concentrations. Qiu *et al.* investigated the impact of the ethanol-to-water ratio on the stability of nanobubbles and found that the number of nanobubbles reached a maximum when the ratio was approximately 1:10 (v/v) [72]. Compared to electrolysis, and Cavitation, the solvent method for generating MNBs offers greater cost advantages. However, this method is typically limited to the production of small quantities of MNBs and struggles with controlling the size distribution of the bubbles.

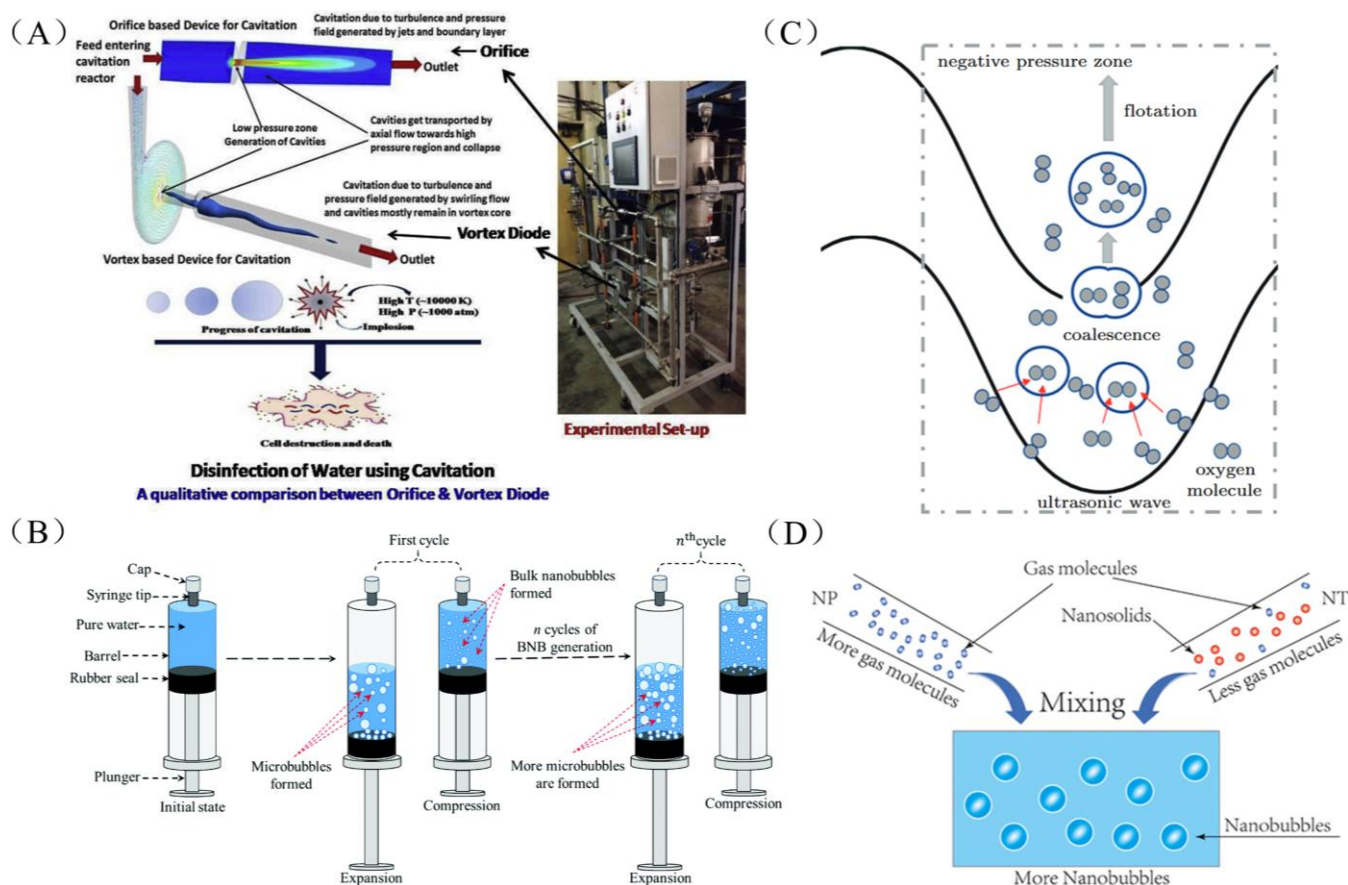


**Figure 3:** (A) Experimental set-up and schematic of disinfection using cavitation [64]; (B) Schematic diagram of MNBs generation process by a continuous expansion-compression cycle of pure water in a syringe [65]; (C) The mechanism of MNBs generation by ultrasonic method [24]; and (D) The generation of MNBs by solvent exchange method [26].

### 3.2. Characterization Techniques for MNBs

After the generation of MNBs within a solution, subsequent analysis of their properties, such as quantitative, size distribution, and surface characteristics, is essential for optimizing their use in catalytic reactions. Consequently, this section primarily focuses on introducing characterization methods for properties of MNBs, including Optical microscope, Dynamic Light Scattering (DLS), Nanoparticle Tracking Analysis (NTA), Total-Internal-Reflection-Fluorescence Microscopy (TIRFM) Excitation, Cryo-Transmission Electron Microscopy (cryo-TEM), Atomic Force Microscope (AFM), Optical Flow Cytometry, Resonant Mass Measurements (RMM), Zeta potential, and Synchrotron-based Scanning Transmission X-ray Microscopy (STXM). The corresponding information are compiled in Table 1, along with a discussion on the structural properties they examine, the detection principles, and the merits and demerits associated with each technique. The information obtained from these analyses aids in comprehending the influence and behavior mechanisms of MNBs in catalytic reactions, providing guidance for optimizing the properties of MNBs to enhance catalytic efficiency.

## 4. The Application of MNBs in Wastewater Treatment

### 4.1. The Application in Catalytic Ozonation

Ozone oxidation is extensively utilized in the remediation of organic pollutants in wastewater due to its high oxidative capacity and the minimal generation of secondary by-products [87, 88]. Despite these advantages, the dissolution of ozone gas in water is constrained by a poor gas-liquid mass transfer coefficient, which hinders the



**Table1: The characterization techniques for MNBs.**

Characterization Techniques	The Detected Structure and Properties	Detection Principles	Advantages	Disadvantages	Ref.
Optical microscope	The morphology and dynamics of MNBs	Direct optical imaging (DOD)	The morphology and dynamics of MNBs can be observed directly	Some optical imaging still requires higher resolution, while some technologies have other limitations such as laser speckle.	[74-76]
Dynamic Light Scattering (DLS)	Grain size distribution	Analyzing MNBs size distribution by measuring the intensity fluctuations of light scattered by nanoparticles in a sample	Fast, non-destructive and easy to operate	The results may fluctuate somewhat due to the Brownian motion of the MNBs, making it difficult to obtain the specific motion of each bubble	[72, 77, 78]
Nanoparticle Tracking Analysis (NTA)	MNBs size, concentration, trajectory	Tracking the motion of nanobubbles in a small volume using light scattering to count MNBs size and concentration	Real-time tracking of MNBs trajectories to analyze particle size and concentration; this method is suitable for low-concentration MNBs analysis	The equipment is costly and requires specialized operation	[10, 68, 79]
Total-Internal-Reflection-Fluorescence Microscopy (TIRFM) Excitation	The size and motion of MNBs	Total internal reflection, generation of fading wave, fluorescence excitation, and fluorescence detection	Able to detect the mechanical strength of MNBs, fast measurement, simple sample preparation	Unintuitive data output, only suitable for bulk MNBs, poor chemical sensitivity	[29, 76]
Cryo-Transmission Electron Microscopy (cryo-TEM)	Morphology, size, distribution and possible internal structure	A sample of amorphous ice-encapsulated MNBs was formed by rapidly freezing water samples to liquid nitrogen temperatures, and then imaged using a transmission electron beam at very low temperatures	<ol style="list-style-type: none"> <li>1. Provides nanometer or even sub-nanometer resolution, clearly demonstrating the fine structure of MNBs</li> <li>2. Fast freezing technology helps to reduce the deformation and damage of the sample during the preparation process</li> <li>3. The electron beam causes less radiation damage to the sample at low temperatures, which helps to get more realistic imaging results</li> </ol>	<ol style="list-style-type: none"> <li>1. The sample preparation and imaging process is relatively complex, requiring specialized technical and equipment</li> <li>2. Due to the difficulty of fixing MNBs directly on the sample stage, special sample preparation techniques are required, such as the use of ultrathin carbon film support</li> <li>3. The equipment is expensive and the maintenance cost is high, which restricts the wide application of this method than routine screening</li> </ol>	[29, 80]
Atomic Force Microscope (AFM)	Morphology and surface properties	Scanning of the sample surface using a probe on a microcantilever, imaging by measuring the interaction force between the probe and the sample surface	High resolution, capable of observing nanoscale structures	Complex operation, slow scanning speed, high sample preparation requirements	[77, 81-83]
Optical Flow Cytometry	Size distribution and concentration	In the optical flow cytometry, a narrow hydrodynamic focusing liquid passes through an optical detector at a high speed. The detector is placed at a certain angle with the illumination beam, and particles are calculated one by one via scattering light	High sensitivity and repeatability, fast, real-time (in-situ) and nonintrusive measurement, simple sample preparation, high throughput	Limited resolution (>300 nm), only suitable for bulk MNBs, poor chemical sensitivity	[29, 84]

Resonant Mass Measurements (RMM)	Particle size and concentration	When a liquid flows through a suspended microchannel, mass change of the contained particles/MNBs will alter the resonance frequency of the detector. By knowing the density and flow rate of the liquid, RMM is cable of probing gas density and concentration of MNBs	Better accuracy than DLS, fast, real-time (in-situ) and nonintrusive measurement, simple sample preparation, able to distinguish NBs from NPs	Unavailable for ultrafine NBs, only suitable for bulk MNBs, poor chemical sensitivity	[85]
Electrophoretic measurement of Zeta potential	Zeta-potential	Measuring the surface potential of nanobubbles using their electrophoretic motion in an electric field	High sensitivity and repeatability, fast, real-time (in-situ) and nonintrusive measurement, simple sample preparation	Only suitable for bulk MNBs, sensitive to pH and salt concentrations in solution	[29, 86]
Synchrotron-based Scanning Transmission X-ray Microscopy (STXM)	Shape and size, internal structure and chemical composition	The technique is mainly based on the interaction of matter with X-rays, in particular Near Edge Absorption Fine Structure (NEXAFS) spectroscopy. When soft X-rays penetrate MNBs and their surrounding aqueous environment, gas molecules and water molecules absorb X-rays of a specific energy and produce a specific absorption spectrum	1. STXM technology has extremely high spatial resolution, usually up to tens of nanometers or even higher, which makes it possible to clearly observe the morphology and distribution of MNBs 2. STXM technology can obtain the required information without destroying MNBs 3. STXM is highly sensitive to weak signals in the sample, and is able to detect small changes such as the high-density state of gas molecules inside the MNBs	Complex and expensive equipment, complicated data analysis and complex operation	[82]

catalytic efficiency of the ozonation process. To address this limitation, a multitude of researchers have turned their attention to integrating ozonation with MNBs technology [18, 49, 89, 90]. Kalogerakis *et al.* employed ozone MNBs for the remediation of borehole water in the Rusgenot company located in Western Cape province of South Africa (Fig. 4), and the water quality was significantly improved after treatment. The concentration of Fe decreased from above 2000  $\mu\text{g/L}$  to <200  $\mu\text{g/L}$ , total coliforms decreased from >400 cfu/100 mL to <10 cfu/100 mL, and *E. coli* decreased from >100 cfu/100 mL to <1 cfu/100 mL [91].



**Figure 4:** (A) Raw water tank, treated water tank, sand filters, and MK3 nanobubble generator + ozone generator and (B) visual characteristics of raw and treated borehole water [91].

It is generally considered that this integrated approach can significantly enhance the mass transfer efficiency, therefore promoting catalytic process. For example, Hu *et al.* reported that the peak value of dissolved ozone concentration in the presence of MNBs was about 10 mg/L, which was approximately 15-folds than that in the presence of millimeter bubbles. Owing to the enhanced dissolution of ozone, ozone MNBs can achieve in situ remediation of trichloroethylene-contaminated groundwater. To be specific, the initial concentration of trichloroethylene at well #1, #2, #3, #4, and #5 was 3.529 mg/L, 4.502 mg/L, 10.130 mg/L, 0.264 mg/L, and 2.129 mg/L, respectively. After 6 days of operation from 09:00 to 18:00 local time, the concentration of trichloroethylene at well #1, #2, #3, #4, and #5 decreased to 0.010 mg/L, 0.003 mg/L, 0.018 mg/L, 0.007 mg/L, and 0.003 mg/L, respectively [19]. Similarly, Zhao *et al.* found that the higher specific surface area positively impacted the ozone transfer at the gas-liquid interface [18].

Except for enhancing ozone transfer rate, it has also been proposed that the ozone molecules in the MNBs will be compressed into the condensed phase (~ 50 atm). During the shrinkage and collapse of the MNBs, the highly reactive ozone molecules in the condensed gas phase may react with the large number of hydroxyl that accumulate at the gas-liquid interface, leading to the production of  $\bullet\text{OH}$  (Fig. 5A) [92]. For example, Koundle *et al.* demonstrated that ozone nanobubbles can improve the degradation efficiency of methylene blue under high salinity conditions by enhancing ozone mass transfer efficiency and  $\bullet\text{OH}$  yield [93]. In another case, Soyluoglu *et al.* found that the concentration of  $\bullet\text{OH}$  in conventional ozonation (~ 18000 nM) was much lower than that in ozone nanobubbles solution (27000 nM). However, they proposed that nanobubbles collapse was not the primary mechanism responsible for the continued formation of  $\bullet\text{OH}$  owing to the stability of ozone nanobubbles observed during the reaction [49]. The above studies indicate that the combination of ozone with MNBs technology holds promise as a wastewater treatment technology. However, there are still controversial issues, such as the underlying mechanism of  $\bullet\text{OH}$  generation. Further studies are needed to elucidate these aspects to facilitate the application of MNBs-based ozonation technology in wastewater remediation.

## 4.2. The Application in Fenton-like Process

Fenton-like reactions, which involve the generation of ROS such as  $\bullet\text{OH}$ ,  $\text{O}_2^{\bullet-}$ , or  $^1\text{O}_2$  through the activation of  $\text{H}_2\text{O}_2$  or persulfates, have been extensively utilized for the degradation of organic pollutants in wastewater [94-96]. Recently, researchers have discovered that the integration of MNBs with Fenton-like reactions could potentially enhance mass transfer efficiency and enhance the generation of  $\bullet\text{OH}$ , thereby increasing catalytic performance [33, 97-99].

Ma *et al.* conducted a comparative analysis of the degradation efficiency of Congo red in three different systems: the conventional Fenton process (22.4%), a combined system of Fenton and MNBs (94.4%), and MNBs alone (15.4%). The superior catalytic performance observed in the combined system was attributed to the enhanced generation of  $\bullet\text{OH}$ , since both the reaction between  $\text{Fe}^{2+}$  and  $\text{H}_2\text{O}_2$ , and pyrolysis of water molecules during the collapse of MNBs generated  $\bullet\text{OH}$ . The results of economic analysis showed that the total treatment cost of the coupling system was approximately 13% of the cost of traditional Fenton system [22]. Duan *et al.* revealed that the hydroxyl over MNBs surface could react with  $\text{Mn(IV)=O}$  over  $\text{MnO}_2$ -modified ceramic membranes surface and result in the formation of  $\text{MNBs-O}^{\bullet}$ , which further reacted with  $\text{H}_2\text{O}$  molecules on the gas-liquid interface and generated  $\bullet\text{OH}$ . Meanwhile,  $\text{H}^+$  hydrolyzed by  $\text{H}_2\text{O}_2$  may induce the collapse of  $\text{O}_2$  MNBs and therefore lead to the generation of ROS (Fig. 5B) [99]. Besides, Chen *et al.* found that the high-temperature and high-pressure environment generated by the collapse of MNBs can activate  $\text{H}_2\text{O}_2$  to obtain a higher number of  $\bullet\text{OH}$  [100], but the underlying mechanisms remains to be further clarified. It is also worth noting that most of the current studies have focused on studying the effect of MNBs on  $\bullet\text{OH}$  in the Fenton-like system, while few studies have focused on the effect on other ROS, such as  $\text{O}_2^{\bullet-}$  and  $^1\text{O}_2$ , which need to be further investigated to offer more opportunities.

## 4.3. The Application in Photocatalytic Process

The principle of photocatalytic technology is based on the absorption of photons with energy equal to or exceeding the bandgap width by semiconductor materials. This absorption leads to the excitation and generation of electrons ( $e^-$ )- holes ( $h^+$ ) pairs, which subsequently react with oxygen and water in the medium to produce ROS

such as  $\cdot\text{OH}$  and  $\text{O}_2^{\cdot-}$  [101-103]. Despite the substantial potential of photocatalytic technology in the water treatment domain, attributed to its environmental sustainability and harnessing of renewable energy sources, it encounters challenges in practical applications, such as insufficient light absorption by photocatalysts, constrained oxygen supply, and suboptimal charge separation efficiency. With the development of MNBs technology, numerous researchers have begun to employ MNBs to address several challenges associated with photocatalytic processes in recent years [47, 104, 105].

Fan *et al.* revealed that MNBs induced a unique light scattering effect within  $\text{TiO}_2$  suspensions, which increased the optical path length and consequently enhanced the absorption of light by  $\text{TiO}_2$  (Fig. 5C). Furthermore, MNBs can elevate the dissolved oxygen concentration in water, thereby supplying more oxygen for the photocatalytic reaction and promoting the generation of ROS, synergistically improving the photocatalytic efficiency [45]. They also discovered that the interfacial photoelectric effect induced by MNBs contributed to the accelerated separation of photogenerated  $e^-$  and  $h^+$ , thereby enhancing the photocatalytic performance [38]. In addition, MNBs have also been utilized to enhance the efficiency of visible light photocatalytic water disinfection and sterilization (Fig. 5D) [17, 43]. For instance, a study has proposed and evaluated a novel visible light photocatalytic water disinfection technology through the close coupling with MNBs. The results showed that the inactivation rate constant of *Bacillus subtilis* spores in the coupling system was  $1.28 \text{ h}^{-1}$ , a value 5.6-fold higher than the rate recorded without the use of MNBs. The enriched oxygen content in solution and increased light absorption of  $\text{Ag}/\text{TiO}_2$  was mainly responsible for the enhanced photocatalytic performance [17].

The application of MNBs in photocatalytic process has demonstrated the potential to enhance reaction efficiency, yet some underlying mechanisms are not fully understood. Current challenges include comprehending how MNBs influence the separation and transfer of photogenerated charge carriers, as well as the impact mechanisms of MNBs on the light scattering effects during photocatalytic reactions. Further investigation into these mechanisms is needed to fully harness the application potential of MNBs in the field of photocatalysis.

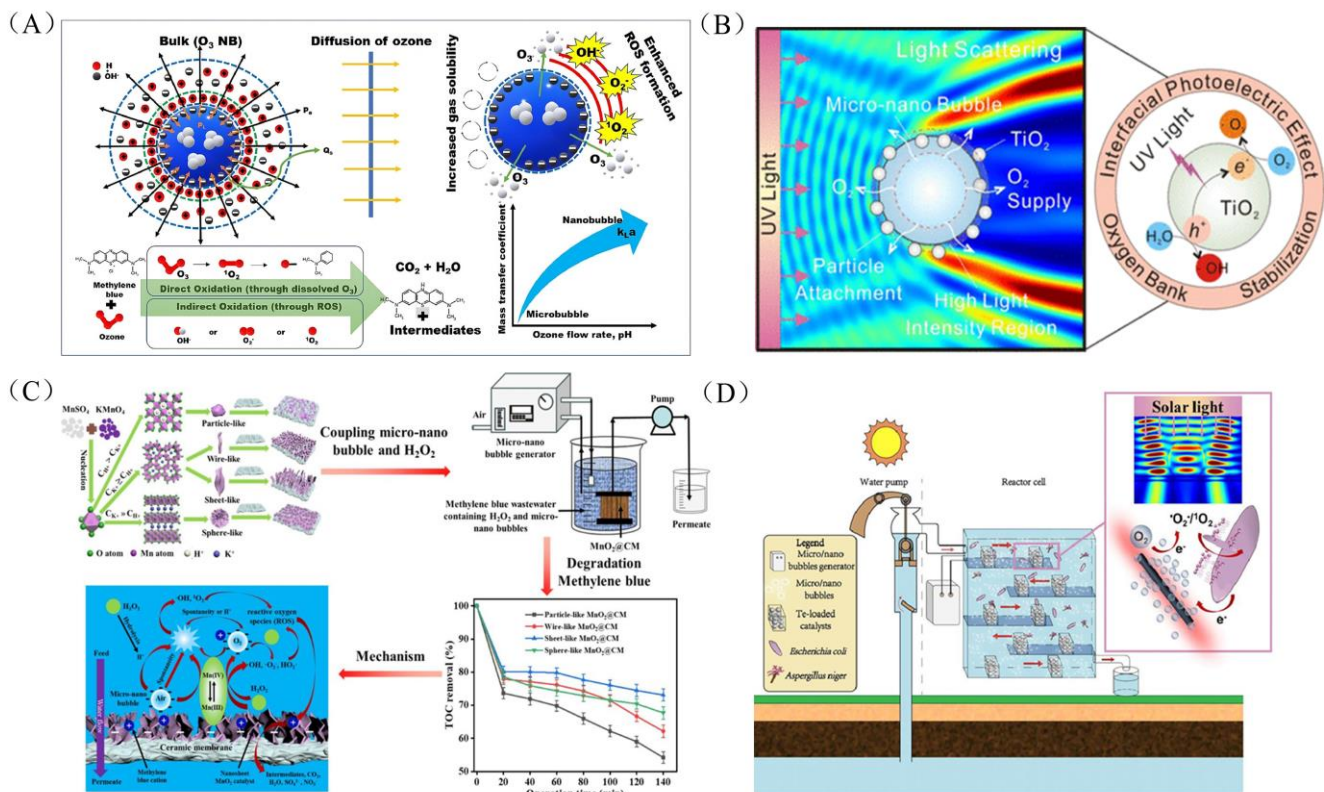


**Figure 5:** (A) The mechanisms of  $\cdot\text{OH}$  production by ozone MNBs in water [92]; (B) The experimental setup and mechanism analysis in  $\text{MnO}_2$ -modified ceramic membrane/ $\text{H}_2\text{O}_2$  system [99]; (C) Mechanism analysis in photocatalytic system coupling MNBs and  $\text{TiO}_2$  [45]; and (D) The procedures and mechanism analysis of MNBs enhancing photocatalytic water disinfection and sterilization efficiency [43].

## 4. Conclusions

The application of MNBs in AOPs is essential to promote the development of green, economic, and efficient technology for wastewater treatment, therefore, it is necessary to have a comprehensive understanding of the properties, generation and utilization of MNBs in AOPs. In this case, this review first briefly discusses the characteristics of MNBs that may have a significant impact on the catalytic efficiency of AOPs. The advantages and disadvantages of commonly used generation methods and characterization methods for MNBs are then discussed to facilitate the selection of appropriate methods. Besides, the potential applications of MNBs in catalyzing ozone, Fenton-like processes and photocatalysis are summarized. Based on the current studies, the existing challenges and recommendations for further researches are presented.

Firstly, many methods (i.e., electrolysis, cavitation, and solvent exchange) have been reported for the preparation of MNBs nowadays, among which hydrodynamic cavitation is a promising method to realize the industrial production of MNBs due to its low operating cost and not easy to be clogged. However, the MNBs prepared by this method usually suffer from inhomogeneous bubble size distribution, which still needs to be improved to enhance the homogeneity and control the bubble size in future studies.

Secondly, although the properties of MNBs are well known, how these properties affect the catalytic efficiency of AOPs is still controversial and needs to be further investigated. For example, does MNBs collapse promote the generation of ROS? Whether this promotion comes from the high-temperature and high-pressure environment generated during the collapse or from the high density of ions (most likely hydroxyl) accumulated around the MNBs interface? The study of these intrinsic mechanisms is crucial for the rational utilization of MNBs to improve the efficiency of AOPs. Moreover, for the application of MNBs in photocatalytic processes, it is also significant to study the mechanism of the light scattering effects of MNBs on the light absorption efficiency and generation and separation of photogenerated charge carriers.

Thirdly, there is still a lack of data on the “safety” of MNBs, which is one of the foundations for their widespread use. Therefore, in future work, it is recommended that an environmental impact assessment of MNBs be carried out, including their impacts on ecosystems and human health, as well as their long-term effects on the environment.

## Conflict of Interest

The authors declare that they have no conflict of interest.

## Funding

This work was financially supported by the National Natural Science Foundation of China (No: 22136003, 22206188, 22476110), Supported by Hubei Provincial Natural Science Foundation of China (No:8246106).

## Acknowledgments

Authors would like to acknowledge financial support by the National Natural Science Foundation and Provincial Natural Science Foundation of China.

## References

- [1] Huo X, Yi H, Almatrafi E, Ma D, Fu Y, Qin L, *et al.* Insights into Fenton-like oxidation of oxytetracycline mediated by Fe-doped porous g-C<sub>3</sub>N<sub>4</sub> nanomaterials: synthesis, performance and mechanism. *Environ Sci: Nano.* 2023; 10: 1828-41. <https://doi.org/10.1039/D3EN00108C>
- [2] Jin L, Huang Y, Liu H, Ye L, Liu X, Huang D. Efficient treatment of actual glyphosate wastewater via non-radical Fenton-like oxidation. *J Hazard Mater.* 2024; 463: 132904. <https://doi.org/10.1016/j.jhazmat.2023.132904>
- [3] Chen Z, Lin B, Huang Y, Liu Y, Wu Y, Qu R, *et al.* Pyrolysis temperature affects the physiochemical characteristics of lanthanum-modified biochar derived from orange peels: Insights into the mechanisms of tetracycline adsorption by spectroscopic analysis and theoretical calculations. *Sci Total Environ.* 2023; 862: 160860. <https://doi.org/10.1016/j.scitotenv.2022.160860>

- [4] Shi Y, Li J, Huang D, Wang X, Huang Y, Chen C, *et al.* Specific adsorption and efficient degradation of cylindrospermopsin on oxygen-vacancy sites of BiOBr. *ACS Catal.* 2023; 13(1): 445-58. <https://doi.org/10.1021/acscatal.2c04228>
- [5] Jioui I, Abrouki Y, Aboul Hrouz S, Sair S, Dânoun K, Zahouily M. Efficient removal of Cu<sup>2+</sup> and methylene blue pollutants from an aqueous solution by applying a new hybrid adsorbent based on alginate-chitosan and HAP derived from Moroccan rock phosphate. *Environ Sci Pollut R.* 2023; 30(49): 107790-810. <https://doi.org/10.1007/s11356-023-29890-y>
- [6] Abrouki Y, Mabrouki J, Anouzla A, Rifi SK, Zahiri Y, Nehhal S, *et al.* Optimization and modeling of a fixed-bed biosorption of textile dye using agricultural biomass from the Moroccan Sahara. *Desalin Water Treat.* 2021; 240: 144-51. <https://doi.org/10.5004/dwt.2021.27704>
- [7] Sakr M, Mohamed MM, Maraqa MA, Hamouda MA, Aly Hassan A, Ali J, *et al.* A critical review of the recent developments in micro-nano bubbles applications for domestic and industrial wastewater treatment. *Alex Eng J.* 2022; 61(8): 6591-612. <https://doi.org/10.1016/j.aej.2021.11.041>
- [8] Patel AK, Singhanian RR, Chen CW, Tseng YS, Kuo CH, Wu CH, *et al.* Advances in micro- and nano bubbles technology for application in biochemical processes. *Environ Technol Inno.* 2021; 23: 101729. <https://doi.org/10.1016/j.eti.2021.101729>
- [9] Ning R, Yu S, Li L, Snyder SA, Li P, Liu Y, *et al.* Micro and nanobubbles-assisted advanced oxidation processes for water decontamination: The importance of interface reactions. *Water Res.* 2024; 265: 122295. <https://doi.org/10.1016/j.watres.2024.122295>
- [10] Azevedo A, Oliveira H, Rubio J. Bulk nanobubbles in the mineral and environmental areas: Updating research and applications. *Adv Colloid Interfac.* 2019; 271: 101992. <https://doi.org/10.1016/j.cis.2019.101992>
- [11] Kim S, Kim H, Han M, Kim T. Generation of sub-micron (nano) bubbles and characterization of their fundamental properties. *Environ Eng Res.* 2018; 24(3): 382-8. <https://doi.org/10.4491/eer.2018.210>
- [12] Moussadiq A, Lazar N-e, Mazkad D, Siro Brigiano F, Baert K, Hauffman T, *et al.* Investigation of electronic and photocatalytic properties of AgTi<sub>2</sub>(PO<sub>4</sub>)<sub>3</sub> NASICON-type phosphate: Combining experimental data and DFT calculations. *J Photoch Photobio A.* 2023; 435: 114289. <https://doi.org/10.1016/j.jphotochem.2022.114289>
- [13] Xie R, Guo K, Li Y, Zhang Y, Zhong H, Leung DYC, *et al.* Harnessing air-water interface to generate interfacial ROS for ultrafast environmental remediation. *Nat Commun.* 2024; 15(1): 8860. <https://doi.org/10.1038/s41467-024-53289-z>
- [14] Luo P, Wang T, Lin F, Luo A, Fiallos M, Ahmed AKA, *et al.* Promoting strategies for biological stability in drinking water distribution system from the perspective of micro-nano bubbles. *Sci Total Environ.* 2024; 954: 176615. <https://doi.org/10.1016/j.scitotenv.2024.176615>
- [15] Zhao Z, Huang X, Zhang Z, Pang H, Wang X, Li P, *et al.* Removal efficiency and mechanism of geosmin by modified micro-nano bubbles in drinking water treatment process. *J Water Process Eng.* 2024; 60: 105125. <https://doi.org/10.1016/j.jwpe.2024.105125>
- [16] Fan W, Desai P, Zimmerman WB, Duan Y, Crittenden JC, Wang C, *et al.* Optical density inferences in aqueous solution with embedded micro/nano bubbles: A reminder for the emerging green bubble cleantech. *J Clean Prod.* 2021; 294: 126258. <https://doi.org/10.1016/j.jclepro.2021.126258>
- [17] Fan W, Cui J, Li Q, Huo Y, Xiao D, Yang X, *et al.* Bactericidal efficiency and photochemical mechanisms of micro/nano bubble-enhanced visible light photocatalytic water disinfection. *Water Res.* 2021; 203: 117531. <https://doi.org/10.1016/j.watres.2021.117531>
- [18] Zhao K, Padervand M, Ren H, Jia T, Guo Q, Yang L, *et al.* Enhancing tetracycline removal efficiency through ozone micro-nano bubbles: Environmental implication and degradation pathway. *ACS EST Engg.* 2024; 4(8): 1860-70. <https://doi.org/10.1021/acsestengg.4c00102>
- [19] Hu L, Xia Z. Application of ozone micro-nano-bubbles to groundwater remediation. *J Hazard Mater.* 2018; 342: 446-53. <https://doi.org/10.1016/j.jhazmat.2017.08.030>
- [20] Movahed SMA, Sarmah AK. Global trends and characteristics of nano- and micro-bubbles research in environmental engineering over the past two decades: A scientometric analysis. *Sci Total Environ.* 2021; 785: 147362. <https://doi.org/10.1016/j.scitotenv.2021.147362>
- [21] Feng J, Song Z, He Q, Wu X, Miao Z. Enhanced degradation of butyl xanthate by hydrogen peroxide and persulfate using micro-nano bubble. *Miner Eng.* 2024; 218: 108996. <https://doi.org/10.1016/j.mineng.2024.108996>
- [22] Ma P, Han C, He Q, Miao Z, Gao M, Wan K, *et al.* Oxidation of Congo red by Fenton coupled with micro and nanobubbles. *Environ Technol.* 2023; 44(17): 2539-48. <https://doi.org/10.1080/09593330.2022.2036245>
- [23] Bu X, Alheshibri M. The effect of ultrasound on bulk and surface nanobubbles: A review of the current status. *Ultrason Sonochem.* 2021; 76: 105629. <https://doi.org/10.1016/j.ultsonch.2021.105629>
- [24] Mo CR, Wang J, Fang Z, Zhou LM, Zhang LJ, Hu J. Formation and stability of ultrasonic generated bulk nanobubbles. *Chinese Phys B.* 2018; 27(11): 118104. <https://doi.org/10.1088/1674-1056/27/11/118104>
- [25] Angulo A, van der Linde P, Gardeniers H, Modestino M, Fernández Rivas D. Influence of bubbles on the energy conversion efficiency of electrochemical reactors. *Joule.* 2020; 4(3): 555-579. <https://doi.org/10.1016/j.joule.2020.01.005>
- [26] Xiao W, Wang X, Zhou L, Zhou W, Wang J, Qin W, *et al.* Influence of mixing and nanosolids on the formation of nanobubbles. *J Phys Chem B.* 2019; 123(1): 317-23. <https://doi.org/10.1021/acs.jpcc.8b11385>
- [27] Wang B, Su H, Zhang B. Hydrodynamic cavitation as a promising route for wastewater treatment - A review. *Chem Eng J.* 2021; 412: 128685. <https://doi.org/10.1016/j.cej.2021.128685>
- [28] Foudas AW, Kosheleva RI, Favvas EP, Kostoglou M, Mitropoulos AC, Kyzas GZ. Fundamentals and applications of nanobubbles: A review. *Chem Eng Res Des.* 2023; 189: 64-86. <https://doi.org/10.1016/j.cherd.2022.11.013>
- [29] Jia J, Zhu Z, Chen H, Pan H, Jiang L, Su W-H, *et al.* Full life cycle of micro-nano bubbles: Generation, characterization and applications. *Chem Eng J.* 2023; 471: 144621. <https://doi.org/10.1016/j.cej.2023.144621>

- [30] Haris S, Qiu X, Klammler H, Mohamed MMA. The use of micro-nano bubbles in groundwater remediation: A comprehensive review. *Groundw Sustain Dev.* 2020; 11: 100463. <https://doi.org/10.1016/j.gsd.2020.100463>
- [31] Atkinson AJ, Apul OG, Schneider O, Garcia-Segura S, Westerhoff P. Nanobubble technologies offer opportunities to improve water treatment. *Acc Chem Res.* 2019; 52(5): 1196-205. <https://doi.org/10.1021/acs.accounts.8b00606>
- [32] Jia M, Farid MU, Kharraz JA, Kumar NM, Chopra SS, Jang A, *et al.* Nanobubbles in water and wastewater treatment systems: Small bubbles making big difference. *Water Res.* 2023; 245: 120613. <https://doi.org/10.1016/j.watres.2023.120613>
- [33] Marcelino KR, Ling L, Wongkiew S, Nhan HT, Surendra KC, Shitanaka T, *et al.* Nanobubble technology applications in environmental and agricultural systems: Opportunities and challenges. *Crit Rev Environ Sci Technol.* 2023; 53(14): 1378-1403. <https://doi.org/10.1080/10643389.2022.2136931>
- [34] Soyluoglu M, Kim D, Zaker Y, Karanfil T. Stability of oxygen nanobubbles under freshwater conditions. *Water Res.* 2021; 206: 117749. <https://doi.org/10.1016/j.watres.2021.117749>
- [35] Gao Z, Wu W, Sun W, Wang B. Understanding the stabilization of a bulk nanobubble: A molecular dynamics analysis. *Langmuir.* 2021; 37(38): 11281-11291. <https://doi.org/10.1021/acs.langmuir.1c01796>
- [36] Prakash R, Lee J, Moon Y, Pradhan D, Kim SH, Lee HY, *et al.* Experimental investigation of cavitation bulk nanobubbles characteristics: Effects of pH and surface-active agents. *Langmuir.* 2023; 39(5): 1968-1986. <https://doi.org/10.1021/acs.langmuir.2c03027>
- [37] Zhang Z, Li J, Jiang Y, Zhao L, Bai L, Yang J, *et al.* Emission characteristics of aerosols generated during the micro-nano bubble aeration process in wastewater. *Environ Sci Technol.* 2024; 58(39): 17396-405. <https://doi.org/10.1021/acs.est.4c00986>
- [38] Fan W, Zhou Z, Wang W, Huo M, Zhang L, Zhu S, *et al.* Environmentally friendly approach for advanced treatment of municipal secondary effluent by integration of micro-nano bubbles and photocatalysis. *J Clean Prod.* 2019; 237: 117828. <https://doi.org/10.1016/j.jclepro.2019.117828>
- [39] Zhou L, Wang X, Shin H-J, Wang J, Tai R, Zhang X, *et al.* Ultrahigh density of gas molecules confined in surface nanobubbles in ambient water. *J Am Chem Soc.* 2020; 142(12): 5583-93. <https://doi.org/10.1021/jacs.9b11303>
- [40] Shi W, Pan G, Chen Q, Song L, Zhu L, Ji X. Hypoxia remediation and methane emission manipulation using surface oxygen nanobubbles. *Environ Sci Technol.* 2018; 52(15): 8712-7. <https://doi.org/10.1021/acs.est.8b02320>
- [41] Xiang P, Ma P, He Q, Song Z, Miao Z. Enhanced removal of phenol and chemical oxygen demand from coking wastewater using micro and nano bubbles: Microbial community and metabolic pathways. *Bioresour Technol.* 2024; 394: 130207. <https://doi.org/10.1016/j.biortech.2023.130207>
- [42] Churnside JH. Lidar signature from bubbles in the sea. *Opt Express.* 2010; 18(8): 8294-9. <https://doi.org/10.1364/OE.18.008294>
- [43] Ma D, Yin R, Liang Z, Liang Q, Xu G, Lian Q, *et al.* Photo-sterilization of groundwater by tellurium and enhancement by micro/nano bubbles. *Water Res.* 2023; 233: 119781. <https://doi.org/10.1016/j.watres.2023.119781>
- [44] Kim H, Chang JH. Increased light penetration due to ultrasound-induced air bubbles in optical scattering media. *Sci Rep.* 2017; 7(1): 16105. <https://doi.org/10.1038/s41598-017-16444-9>
- [45] Fan W, Li Y, Wang C, Duan Y, Huo Y, Januszewski B, *et al.* Enhanced photocatalytic water decontamination by micro-nano bubbles: Measurements and mechanisms. *Environ Sci Technol.* 2021; 55(10): 7025-7033. <https://doi.org/10.1021/acs.est.0c08787>
- [46] Zhang W, Xiong J, Lin X, Liu Y, Gan T, Hu H, *et al.* Advanced pyro-/piezoelectric catalytic disinfection of water via porous spontaneously polarized ceramic with strong local electric field induced by micro-nano bubbles. *Chem Eng J.* 2024; 499: 155958. <https://doi.org/10.1016/j.cej.2024.155958>
- [47] Huang L, Ji X, Nan B, Yang P, Shi H, Wu Y, *et al.* Enhanced photoelectrochemical water oxidation by micro-nano bubbles: Measurements and mechanisms. *J Alloy Compd.* 2023; 965: 171449. <https://doi.org/10.1016/j.jallcom.2023.171449>
- [48] Zhou S, Nazari S, Hassanzadeh A, Bu X, Ni C, Peng Y, *et al.* The effect of preparation time and aeration rate on the properties of bulk micro-nanobubble water using hydrodynamic cavitation. *Ultrason Sonochem.* 2022; 84: 105965. <https://doi.org/10.1016/j.ultsonch.2022.105965>
- [49] Soyluoglu M, Kim D, Karanfil T. Characteristics and stability of ozone nanobubbles in freshwater conditions. *Environ Sci Technol.* 2023; 57(51): 21898-907. <https://doi.org/10.1021/acs.est.3c07443>
- [50] Jadhav AJ, Barigou M. Electrochemically induced bulk nanobubbles. *Ind Eng Chem Res.* 2021; 60(49): 17999-18006. <https://doi.org/10.1021/acs.iecr.1c04046>
- [51] Vogel YB, Evans CW, Belotti M, Xu L, Russell IC, Yu L-J, *et al.* The corona of a surface bubble promotes electrochemical reactions. *Nat Commun.* 2020; 11(1): 6323. <https://doi.org/10.1038/s41467-020-20186-0>
- [52] van der Linde P, Moreno Soto Á, Peñas-López P, Rodríguez-Rodríguez J, Lohse D, Gardeniers H, *et al.* Electrolysis-driven and pressure-controlled diffusive growth of successive bubbles on microstructured surfaces. *Langmuir.* 2017; 33(45): 12873-86. <https://doi.org/10.1021/acs.langmuir.7b02978>
- [53] Zhang Y, Zhu X, Wood JA, Lohse D. Threshold current density for diffusion-controlled stability of electrolytic surface nanobubbles. *P Natl Acad Sci USA.* 2024; 121(21): 2321958121. <https://doi.org/10.1073/pnas.2321958121>
- [54] Liu H, Xie R, Luo Y, Cui Z, Yu Q, Gao Z, *et al.* Dual interfacial engineering of a Chevrel phase electrode material for stable hydrogen evolution at 2500 mA cm<sup>-2</sup>. *Nat Commun.* 2022; 13(1): 6382. <https://doi.org/10.1038/s41467-022-34121-y>
- [55] Li M, Xie P, Yu L, Luo L, Sun X. Bubble engineering on micro-/nanostructured electrodes for water splitting. *ACS Nano.* 2023; 17(23): 23299-316. <https://doi.org/10.1021/acsnano.3c08831>

- [56] Jiang M, Wang H, Li Y, Zhang H, Zhang G, Lu Z, *et al.* Superaerophobic RuO<sub>2</sub>-based nanostructured electrode for high-performance chlorine evolution reaction. *Small*. 2017; 13(4): 1602240. <https://doi.org/10.1002/sml.201602240>
- [57] Wu M, Yuan S, Song H, Li X. Micro-nano bubbles production using a swirling-type venturi bubble generator. *Chem Eng Process*. 2022; 170: 108697. <https://doi.org/10.1016/j.cep.2021.108697>
- [58] Terasaka K, Hirabayashi A, Nishino T, Fujioka S, Kobayashi D. Development of microbubble aerator for waste water treatment using aerobic activated sludge. *Chem Eng Sci*. 2011; 66(14): 3172-9. <https://doi.org/10.1016/j.ces.2011.02.043>
- [59] Liu S, Yuan X, Shao Z, Xiang K, Huang W, Tian H, *et al.* Investigation of singlet oxygen and superoxide radical produced from vortex-based hydrodynamic cavitation: Mechanism and its relation to cavitation intensity. *Sci Total Environ*. 2024; 929: 172761. <https://doi.org/10.1016/j.scitotenv.2024.172761>
- [60] Birkin PR, Linfield S, Youngs JJ, Denuault G. Generation and *in situ* electrochemical detection of transient nanobubbles. *J Phys Chem C*. 2020; 124(13): 7544-9. <https://doi.org/10.1021/acs.jpcc.0c00435>
- [61] Nirmalkar N, Pacek AW, Barigou M. On the Existence and stability of bulk nanobubbles. *Langmuir*. 2018; 34(37): 10964-73. <https://doi.org/10.1021/acs.langmuir.8b01163>
- [62] Roy K, Moholkar VS. Sulfadiazine degradation using hybrid AOP of heterogeneous Fenton/persulfate system coupled with hydrodynamic cavitation. *Chem Eng J*. 2020; 386: 121294. <https://doi.org/10.1016/j.cej.2019.03.170>
- [63] Hong F, Xue H, Yuan X, Wang L, Tian H, Ye L, *et al.* Numerical investigation on the hydrodynamic performance with special emphasis on the cavitation intensity detection in a Venturi cavitator. *Process Saf Environ*. 2023; 175: 212-26. <https://doi.org/10.1016/j.psep.2023.05.037>
- [64] Jain P, Bhandari VM, Balapure K, Jena J, Ranade VV, Killedar DJ. Hydrodynamic cavitation using vortex diode: An efficient approach for elimination of pathogenic bacteria from water. *J Environ Manage*. 2019; 242: 210-9. <https://doi.org/10.1016/j.jenvman.2019.04.057>
- [65] Ferraro G, Jadhav AJ, Barigou M. A Henry's law method for generating bulk nanobubbles. *Nanoscale*. 2020; 12(29): 15869-79. <https://doi.org/10.1039/D0NR03332D>
- [66] Wang Q, Zhao H, Qi N, Qin Y, Zhang X, Li Y. Generation and stability of size-adjustable bulk nanobubbles based on periodic pressure change. *Sci Rep*. 2019; 9(1): 1118. <https://doi.org/10.1038/s41598-018-38066-5>
- [67] Kim JY, Song MG, Kim JD. Zeta Potential of nanobubbles generated by ultrasonication in aqueous alkyl polyglycoside solutions. *J Colloid Interf Sci*. 2000; 223(2): 285-91. <https://doi.org/10.1006/jcis.1999.6663>
- [68] Yasuda K, Matsushima H, Asakura Y. Generation and reduction of bulk nanobubbles by ultrasonic irradiation. *Chem Eng Sci*. 2019; 195: 455-61. <https://doi.org/10.1016/j.ces.2018.09.044>
- [69] Cho SH, Kim JY, Chun JH, Kim JD. Ultrasonic formation of nanobubbles and their zeta-potentials in aqueous electrolyte and surfactant solutions. *Colloid Surface A*. 2005; 269(1): 28-34. <https://doi.org/10.1016/j.colsurfa.2005.06.063>
- [70] Jadhav AJ, Barigou M. Bulk nanobubbles or not nanobubbles: That is the question. *Langmuir*. 2020; 36(7): 1699-1708. <https://doi.org/10.1021/acs.langmuir.9b03532>
- [71] Li C, Li X, Xu M, Zhang H. Effect of ultrasonication on the flotation of fine graphite particles: Nanobubbles or not? *Ultrason Sonochem*. 2020; 69: 105243. <https://doi.org/10.1016/j.ultsonch.2020.105243>
- [72] Qiu J, Zou Z, Wang S, Wang X, Wang L, Dong Y, *et al.* Formation and stability of bulk nanobubbles generated by ethanol-water exchange. *ChemPhysChem*. 2017; 18(10): 1345-50. <https://doi.org/10.1002/cphc.201700010>
- [73] Stride E, Edirisinghe M. Novel microbubble preparation technologies. *Soft Matter*. 2008; 4(12): 2350-9. <https://doi.org/10.1039/b809517p>
- [74] Yu K, Zhang H, Hodges C, Biggs S, Xu Z, Cayre OJ, *et al.* Foaming behavior of polymer-coated colloids: The need for thick liquid films. *Langmuir*. 2017; 33(26): 6528-39. <https://doi.org/10.1021/acs.langmuir.7b00723>
- [75] Zhang W, Wang J, Li B, Yu K, Wang D, Yongphet P, *et al.* Experimental investigation on bubble coalescence regimes under non-uniform electric field. *Chem Eng J*. 2021; 417: 127982. <https://doi.org/10.1016/j.cej.2020.127982>
- [76] Chan CU, Ohl C-D. Total-Internal-Reflection-Fluorescence microscopy for the study of nanobubble dynamics. *Phys Rev Lett*. 2012; 109(17): 174501. <https://doi.org/10.1103/PhysRevLett.109.174501>
- [77] Yu K, Hodges C, Biggs S, Cayre OJ, Harbottle D. Polymer molecular weight dependence on lubricating particle-particle interactions. *Ind Eng Chem Res*. 2018; 57(6): 2131-8. <https://doi.org/10.1021/acs.iecr.7b04609>
- [78] Hassan PA, Rana S, Verma G. Making sense of brownian motion: Colloid characterization by dynamic light scattering. *Langmuir*. 2015; 31(1): 3-12. <https://doi.org/10.1021/la501789z>
- [79] Oh SH, Kim J-M. Generation and stability of bulk nanobubbles. *Langmuir*. 2017; 33(15): 3818-323. <https://doi.org/10.1021/acs.langmuir.7b00510>
- [80] Yu K, Chen L, Zhang W, Zhang H, Jia J, Wang Z, *et al.* Behaviour of polymer-coated composite nanoparticles at bubble-stabilizing interfaces during bubble coarsening and accelerated coalescence: A Cryo-SEM study. *J Colloid Interf Sci*. 2023; 633: 113-9. <https://doi.org/10.1016/j.jcis.2022.11.100>
- [81] Walczyk W, Schönherr H. Characterization of the interaction between AFM tips and surface nanobubbles. *Langmuir*. 2014; 30(24): 7112-26. <https://doi.org/10.1021/la501484p>
- [82] Pan G, He G, Zhang M, Zhou Q, Tyliczcak T, Tai R, *et al.* Nanobubbles at hydrophilic particle-water interfaces. *Langmuir*. 2016; 32(43): 11133-7. <https://doi.org/10.1021/acs.langmuir.6b01483>



- [83] Thi Phan KK, Truong T, Wang Y, Bhandari B. Nanobubbles: Fundamental characteristics and applications in food processing. *Trends Food Sci Tech.* 2020; 95: 118-30. <https://doi.org/10.1016/j.tifs.2019.11.019>
- [84] Eklund F, Alheshibri M, Swenson J. Differentiating bulk nanobubbles from nanodroplets and nanoparticles. *Curr Opin Colloid In.* 2021; 53: 101427. <https://doi.org/10.1016/j.cocis.2021.101427>
- [85] Zhou L, Wang S, Zhang L, Hu J. Generation and stability of bulk nanobubbles: A review and perspective. *Curr Opin Colloid In.* 2021; 53: 101439. <https://doi.org/10.1016/j.cocis.2021.101439>
- [86] Babu KS, Amamcharla JK. Generation methods, stability, detection techniques, and applications of bulk nanobubbles in agro-food industries: a review and future perspective. *Crit Rev Food Sci.* 2023; 63(28): 9262-81. <https://doi.org/10.1080/10408398.2022.2067119>
- [87] Guo Y, Long J, Huang J, Yu G, Wang Y. Can the commonly used quenching method really evaluate the role of reactive oxygen species in pollutant abatement during catalytic ozonation? *Water Res.* 2022; 215: 118275. <https://doi.org/10.1016/j.watres.2022.118275>
- [88] Guo Y, Zhang Y, Yu G, Wang Y. Revisiting the role of reactive oxygen species for pollutant abatement during catalytic ozonation: The probe approach versus the scavenger approach. *Appl Catal B: Environ.* 2021; 280: 119418. <https://doi.org/10.1016/j.apcatb.2020.119418>
- [89] Takahashi M, Ishikawa H, Asano T, Horibe H. Effect of microbubbles on ozonized water for photoresist removal. *J Phys Chem C.* 2012; 116(23): 12578-83. <https://doi.org/10.1021/jp301746g>
- [90] Xie Z, Shentu J, Long Y, Lu L, Shen D, Qi S. Effect of dissolved organic matter on selective oxidation of toluene by ozone micro-nano bubble water. *Chemosphere.* 2023; 325: 138400. <https://doi.org/10.1016/j.chemosphere.2023.138400>
- [91] Kalogerakis N, Kalogerakis GC, Botha QP. Environmental applications of nanobubble technology: Field testing at industrial scale. *Can J Chem Eng.* 2021; 99(11): 2345-54. <https://doi.org/10.1002/cjce.24211>
- [92] Yang X, Chen L, Oshita S, Fan W, Liu S. Mechanism for enhancing the ozonation process of micro- and nanobubbles: Bubble behavior and interface reaction. *ACS EST Water.* 2023; 3(12): 3835-47. <https://doi.org/10.1021/acsestwater.3c00031>
- [93] Koundle P, Nirmalkar N, Momotko M, Boczkaj G. Ozone nanobubble technology as a novel AOPs for pollutants degradation under high salinity conditions. *Water Res.* 2024; 263: 122148. <https://doi.org/10.1016/j.watres.2024.122148>
- [94] Li L, Yin Z, Cheng M, Qin L, Liu S, Yi H, *et al.* Insights into reactive species generation and organics selective degradation in Fe-based heterogeneous Fenton-like systems: A critical review. *Chem Eng J.* 2023; 454: 140126. <https://doi.org/10.1016/j.cej.2022.140126>
- [95] Li L, Cheng M, Almatrafi E, Qin L, Liu S, Yi H, *et al.* Tuning the intrinsic catalytic sites of magnetite to concurrently enhance the reduction of H<sub>2</sub>O<sub>2</sub> and O<sub>2</sub>: Mechanism analysis and application potential evaluation. *J Hazard Mater.* 2023; 457: 131800. <https://doi.org/10.1016/j.jhazmat.2023.131800>
- [96] Liu S, Lai C, Zhou X, Zhang C, Chen L, Yan H, *et al.* Peroxydisulfate activation by sulfur-doped ordered mesoporous carbon: Insight into the intrinsic relationship between defects and <sup>1</sup>O<sub>2</sub> generation. *Water Res.* 2022; 221: 118797. <https://doi.org/10.1016/j.watres.2022.118797>
- [97] Gurung A, Dahl O, Jansson K. The fundamental phenomena of nanobubbles and their behavior in wastewater treatment technologies. *Geosystem Eng.* 2016; 19(3): 133-42. <https://doi.org/10.1080/12269328.2016.1153987>
- [98] Zhang R, Wang J, Yang J, Qin S, Li F, Zhao L, *et al.* Treatment of wastewater-CPL by biochar-based Fenton-like catalyst in the presence of micro-nano bubbles. *Water Air Soil Poll.* 2022; 233(6): 207. <https://doi.org/10.1007/s11270-022-05654-1>
- [99] Duan Y, Zhao D, Liu Z, Yu J. Hydrogen peroxide enhancing the process of MnO<sub>2</sub>-modified ceramic membrane catalyzing micro-nano bubble. *Sep Purif Technol.* 2025; 353: 128320. <https://doi.org/10.1016/j.seppur.2024.128320>
- [100] Chen Z, Fu M, Yuan C, Hu X, Bai J, Pan R, *et al.* Study on the degradation of tetracycline in wastewater by micro-nano bubbles activated hydrogen peroxide. *Environ Technol.* 2022; 43(23): 3580-90. <https://doi.org/10.1080/09593330.2021.1928292>
- [101] Lai C, An N, Li B, Zhang M, Yi H, Liu S, *et al.* Future roadmap on nonmetal-based 2D ultrathin nanomaterials for photocatalysis. *Chem Eng J.* 2021; 406: 126780. <https://doi.org/10.1016/j.cej.2020.126780>
- [102] Zhang M, Lai C, Li B, Xu F, Huang D, Liu S, *et al.* Unravelling the role of dual quantum dots cocatalyst in 0D/2D heterojunction photocatalyst for promoting photocatalytic organic pollutant degradation. *Chem Eng J.* 2020; 396: 125343. <https://doi.org/10.1016/j.cej.2020.125343>
- [103] Wang X, Zhang X, Zhang Y, Wang Y, Sun SP, Wu WD, *et al.* Nanostructured semiconductor supported iron catalysts for heterogeneous photo-Fenton oxidation: a review. *J Mater Chem A.* 2020; 8(31): 15513-46. <https://doi.org/10.1039/D0TA04541A>
- [104] Rojviroon O, Rojviroon T. Photocatalytic process augmented with micro/nano bubble aeration for enhanced degradation of synthetic dyes in wastewater. *Water Resour Ind.* 2022; 27: 100169. <https://doi.org/10.1016/j.wri.2021.100169>
- [105] Boonwan C, Rojviroon T, Rojviroon O, Rajendran R, Paramasivam S, Chinnasamy R, *et al.* Micro-nano bubbles in action: AC/TiO<sub>2</sub> hybrid photocatalysts for efficient organic pollutant degradation and antibacterial activity. *Biocatal Agric Biotechnol.* 2024; 61: 103400. <https://doi.org/10.1016/j.bcab.2024.103400>